

## BIOMINERALIZATION OF $\text{Fe}_3\text{O}_4$ IN BACTERIA

R. B. Frankel and G.C. Papaefthymiou

Francis Bitter National Magnet Laboratory  
Massachusetts Institute of Technology  
Cambridge, MA 02139

### INTRODUCTION

Iron is a constituent of the active sites of many important proteins including hemoglobin and myoglobin, the cytochromes, iron-sulfur proteins, nitrogenase and others. Because of the importance of the iron-containing proteins to the physiology of a wide variety of organisms, their physical and electronic structures have been extensively studied. Since the iron atom or atoms often play a central role in the function of the protein, Mössbauer spectroscopy is one of the most important tools in these studies.

In most cases iron is incorporated as an isolated atom or part of a small cluster of atoms at specific sites and is ligated by oxygen, nitrogen, or sulfur atoms of the polypeptide chain. In these systems the iron atoms are paramagnetic or diamagnetic depending on whether the number of 3d electrons is odd or even. An important exception is the iron storage protein ferritin which can accommodate up to 4000 atoms per molecule. The iron is deposited as a hydrous iron oxide mineral in a spherical cavity in the protein. Exchange interactions between the iron atoms are strong and the mineral is magnetically ordered at low temperature.<sup>1</sup>

In addition to ferritin, and the related iron-storage material hemosiderin, it is now known that organisms including bacteria and higher plants and animals can produce other iron deposits of varying crystallinity.<sup>2</sup> These deposits can occur extracellularly or intracellularly, and include the minerals ferrihydrite, goethite, lepidocrocite, and magnetite. All these minerals are magnetically ordered at low temperature and magnetite is magnetically ordered even at room temperature. The processes by which organisms deposit

iron minerals are interesting because they involve biological intervention in essentially inorganic processes. In discussing biomineralization of calcium and silica as well as iron deposits, Lowenstam<sup>2,3</sup> has distinguished "biological induced" mineralization from "organic matrix-mediated" mineralization. In the former process, cellular export of metabolic end products leads to precipitation of metal ions in the environment. In the latter process, the minerals are deposited in a preformed organic matrix produced by the organism. Biologically induced mineralization results in mineral forms of varying crystallinity with crystal structures and habits similar to those produced by inorganic processes. On the other hand, organic matrix-mediated mineralization typically results in crystals with definite morphologies, narrow size ranges and often, definite orientations in the matrix. Both types of processes might contribute to mineralization in certain cases.

An example of a biologically induced iron mineralization process might be FeS precipitation in marine sediments, resulting from  $S^{=}$  ions produced in the metabolism of sulfate reducing bacteria such as Desulfovibrio. In contrast, magnetotactic bacteria,<sup>4</sup> such as Aquaspirillum magnetotacticum, produce uniformly sized and shaped crystals of  $Fe_3O_4$  in an intracellular sheath. The morphologies of the particles are apparently species specific, indicating a matrix-mediated precipitation process.<sup>5</sup> A possible example of a mixed mineralization process concerns the so-called iron bacteria, such as Leptothrix, which precipitate hydrous iron oxides extracellularly.<sup>6</sup> The precipitate is x-ray amorphous but the precipitation process could involve polysaccharides on the surface of the cells.

#### MÖSSBAUER SPECTROSCOPY OF FERRITIN

The iron core of the protein ferritin is the most extensively studied iron biomineral.<sup>7</sup> Ferritins occur widely in the living world, from bacteria to man. Mammalian ferritin consists of a spherical protein shell with  $\sim 12$  nm outer diameter encasing a 7 nm hydrous iron oxide core which is associated with phosphate. The apoprotein shell consists of 24 identical protein subunits each of molecular weight 18,500. The number of iron atoms in a molecule can vary from zero to approximately 4000. While ferritin is easily crystallized, there is no unique orientation of the hydrous iron oxide cores with respect to the apoferritin shells. Hence, a precise x-ray determination of the crystal structure of the core material has not been possible. However, it has been suggested that the hydrous iron oxide cores of ferritin consist essentially of the mineral ferrihydrite, with six fold oxygen coordinated ferric iron and hexagonal close packing of the oxygen atoms.<sup>8,9</sup>

Iron in ferritins from several sources have been studied by Mössbauer spectroscopy.<sup>1,10-12</sup> The high temperature spectrum ( $T > 60$  K) typically consists of a broadened quadrupole doublet with isomer shift and quadrupole splitting characteristic of  $\text{Fe}^{+3}$ . At helium temperatures ( $T \sim 4.2$  K) the spectrum is magnetically split with a 490 kOe field at the nucleus. The lines are broad and some authors have used a distribution of hyperfine fields to fit the spectra. As the temperature is increased from 4.2 K, the magnetically split spectrum gradually decreases in intensity and the quadrupole doublet increases in intensity. The temperature range over which the magnetically split spectrum and quadrupole doublet coexist depends on the source of the ferritin (mammalian, plant or bacterial in origin) and the degree of iron loading of the ferritin molecules.

The temperature dependence of the Mössbauer spectrum is due to superparamagnetic behavior in the small particles of the ferritin core.<sup>1</sup> In this phenomenon, the iron atoms are antiferromagnetically coupled at low temperature. The sublattice magnetizations lie along particular crystallographic orientations in the crystal, the easy magnetic axes. At finite temperature there is a certain probability that the sublattice magnetizations will undergo a transition to an energetically equivalent easy axis. The sublattice relaxation time  $\tau$  is an exponential function of the magnetic anisotropy  $K$ , the volume  $V$  of the particle, and the temperature:

$$\tau = \tau_0 \cdot \exp [KV/kT] \quad (1)$$

where  $\tau_0$  is a constant and  $k$  is Boltzmann's constant. When the relaxation time in a particle is of the order of or faster than the Larmor precession time of the 14.4 keV excited state, the hyperfine field will be wiped out and the spectrum will consist of the quadrupole doublet. For particles of a given volume, this condition will occur at a definite temperature called the blocking temperature. If there is a distribution of particle volumes in the sample, there will be a distribution of blocking temperatures, and the magnetic spectrum and the quadrupole doublet corresponding to the larger particles and the smaller particles, respectively, can coexist. Determination of the relative intensities of the two subspectra as a function of temperature is a means of measuring the distribution of particle volumes. For example, Williams et al.<sup>12</sup> found that ferritins reconstituted from apoferritin and iron under different conditions (e.g., presence or absence of phosphate) had different distributions of particle volumes.

The spectra of ferritin from the fungus *Phycomyces*<sup>11</sup> and of an unusual bacterial ferritin with associated heme groups from *Azotobacter*<sup>13</sup> are similar to mammalian ferritin except that the superparamagnetic behavior is observed over lower temperature

ranges. If the core compositions in those ferritins are similar to that in the horse spleen ferritin, we can assume that the decreases in the blocking temperatures reflect smaller particle sizes in the plant and bacterial ferritins.

An iron-rich storage material also referred to as bacterial ferritin has been found in E. coli and other prokaryotes.<sup>14</sup> However, the Mössbauer spectra for these materials are distinctly different than the ferritin from Azotobacter. The Mössbauer spectrum for  $T > 4$  K of the ferritin from E. coli is a quadrupole doublet with parameters characteristic of high spin  $\text{Fe}^{3+}$ . A six line magnetic hyperfine spectrum with an effective magnetic field at the nucleus of 430 kOe is observed at  $T < 1$  K. Above 1 K the lines broaden and the splitting decreases with increasing  $T$ , and collapses into the quadrupole doublet at about 3.5 K. Between 1.2 and 3.5 K the doublet and sextet are superposed, indicating a spread of magnetic transition temperatures. This indicates lower energy magnetic interactions between iron atoms than in other ferritins, perhaps reflecting less dense packing of the iron atoms or less crystallinity in the core.

Cohen et al.<sup>15</sup> have discovered an interesting dynamic effect in the Mössbauer spectra of crystals of horse spleen ferritin molecules when the crystals are warmed through the freezing point of water ( $\sim 265$  K). Below 265 K the spectrum consists of the quadrupole doublet referred to above. Above 265 K, the spectrum consists of a narrow line quadrupole doublet superposed on a broad spectrum of width  $\sim 4$  cm/s. This effect has been interpreted in terms of bounded or localized diffusive motions of the ferritin molecules after interstitial water in the crystal has melted. Analysis has been made in terms of discrete transitions between a number of fixed points, or in terms of continuous harmonic motion driven by Brownian forces.<sup>16</sup> For small particles in water, frictional forces are large compared to inertial forces and the situation corresponds to strong overdamping. It has been shown that the theoretical spectrum based on these models does indeed consist of a narrow and a broad component, with parameters determined by a diffusion constant  $D$  and the ratio of harmonic to frictional forces. The intensity of the narrow line and the width of the broad line can be used to calculate the mean squared displacement and the diffusion constant, respectively, of the iron atoms participating in the diffusive motions.

#### MÖSSBAUER SPECTROSCOPY OF MAGNETOTACTIC BACTERIA

Magnetotactic bacteria are various species of aquatic microorganisms that orient and swim along magnetic field lines.<sup>4,17-19</sup> All magnetotactic cells examined to date by electron microscopy contain iron-rich, electron-opaque particles.<sup>4,18,20,21</sup> In several

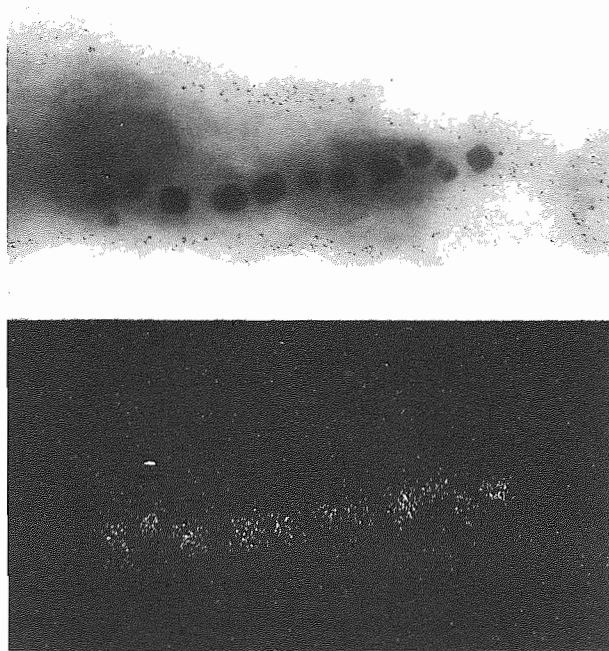


Fig. 1. Transmission electron micrograph of a portion of A. magnetotacticum showing 500 Å  $\text{Fe}_3\text{O}_4$  particles (top). An Fe x-ray pulse map of the same portion of the cell, showing that cellular iron is concentrated in the particles (bottom). (After Ref. 28)

species of magnetotactic bacteria, and possibly all, the particles consist of magnetite,  $\text{Fe}_3\text{O}_4$ .<sup>21,22</sup> Cuboidal, rectangular parallelepiped, and arrow-head shaped particles occur in different species with typical dimensions of 400 to 1200 Å. These are within the single-magnetic-domain size range of  $\text{Fe}_3\text{O}_4$ . In most species the particles are arranged in chains, which impart a magnetic moment of the cell, parallel to the axis of motility. The moment is sufficiently large that the bacterium is oriented in the geomagnetic field at ambient temperature as it swims, i.e., the chain of  $\text{Fe}_3\text{O}_4$  particles functions as a biomagnetic compass.<sup>23</sup> The organism thus propels itself along the geomagnetic field lines. The direction of migration depends on the orientation of the biomagnetic compass. Those with North-seeking pole forward migrate North along the field lines. Those with South-seeking pole forward migrate South. It has been found that North-seeking bacteria predominate in the Northern Hemisphere while South-seeking bacteria predominate in the Southern Hemisphere.<sup>24,25</sup> The vertical component of the inclined geomagnetic field selects the predominant polarity in each hemisphere by presumably favoring those cells whose polarity causes them to be directed downward towards the sediments and away from the toxic effects of the oxygen rich surface waters. At the geomagnetic equator where the vertical component is zero both polarities co-exist;<sup>26</sup> presumably, horizontally directed motion is equally beneficial to both polarities in reducing harmful upward migration.

In the freshwater magnetotactic spirillum, *A. magnetotacticum*, iron comprises 2% or more of the cellular dry weight.<sup>27</sup> Electron microscopy studies of this organism show that the  $\text{Fe}_3\text{O}_4$  particles are cuboidal, 40 - 50 nm in width, and are arranged in a chain that longitudinally traverses the cell (Fig. 1). The particles are enveloped by electron-transparent and electron-dense layers; a particle and its enveloping membrane has been termed a magnetosome.<sup>20</sup>

Since *A. magnetotacticum* is cultured in a chemically defined medium in which iron is available as soluble ferric quinate<sup>27</sup> the presence of intracellular  $\text{Fe}_3\text{O}_4$  implies a process of bacterial precipitation of this mineral, with control of particle size, number and location in the cell.

In order to elucidate the  $\text{Fe}_3\text{O}_4$  biomineralization process, cells and cell fractions, some isotopically enriched in Fe-57, have been studied by Mössbauer spectroscopy.<sup>28</sup> Cells of a non-magnetotactic variant that accumulated iron but did not make  $\text{Fe}_3\text{O}_4$  and of a cloned, nonmagnetotactic strain that accumulated less iron, were also studied. The results suggest that  $\text{Fe}_3\text{O}_4$  is precipitated by reduction of a hydrous ferric-oxide precursor.

Mössbauer spectra of wet packed cells enriched in Fe-57 at 200 and 80 K are shown in Figs. 2 and 3a, respectively. The 200 K spectrum can be analyzed as a superposition of spectra corresponding

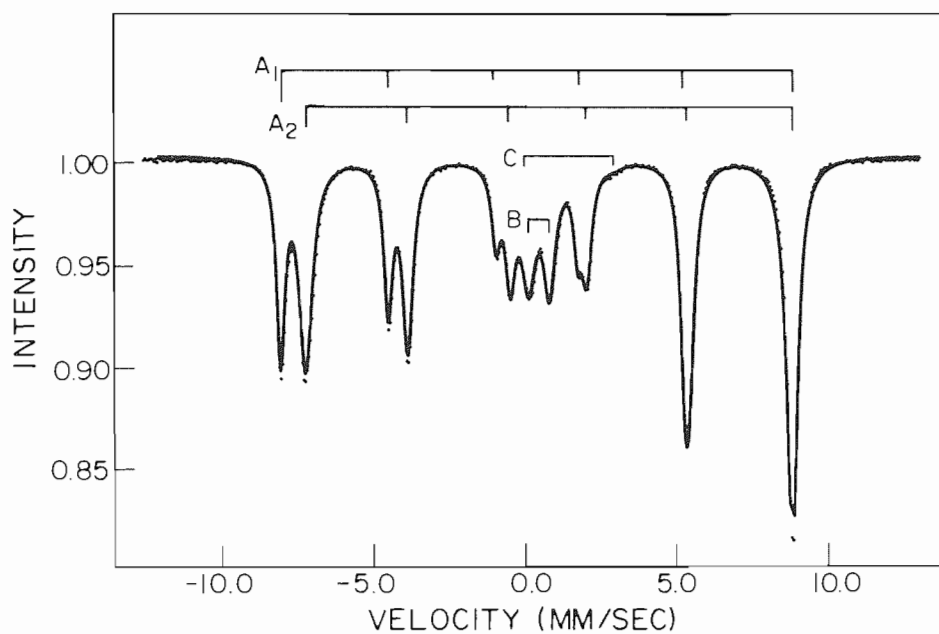


Fig. 2 Mössbauer spectrum of wet, packed cells of *A. magnetotacticum* at 200 K. Subspectra  $A_1$  and  $A_2$  are due to  $\text{Fe}_3\text{O}_4$ ; spectrum B is a ferric doublet; spectrum C is a ferrous doublet. The solid line is a theoretical least-squares fit to the data. (Ref. 28).

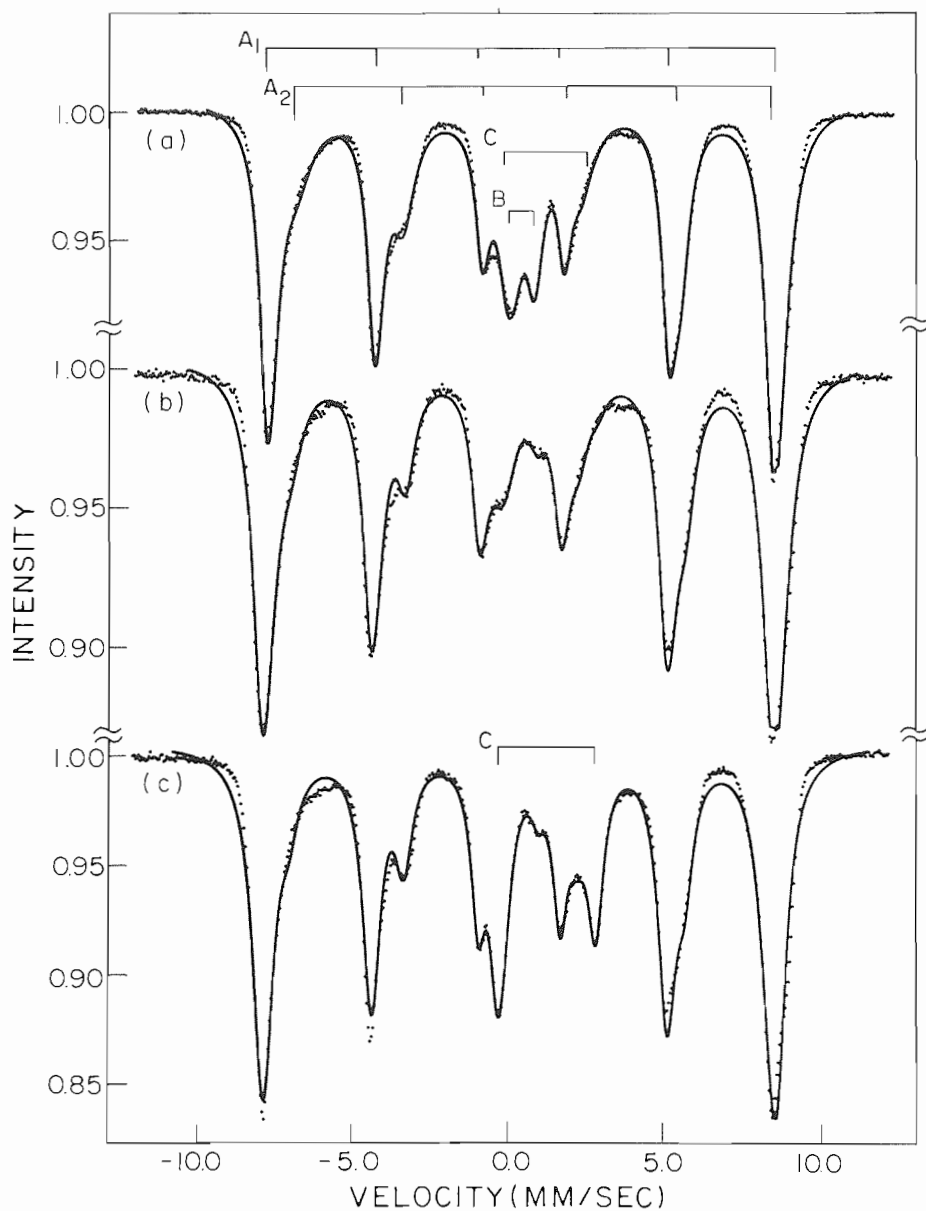


Fig. 3. Mössbauer spectra of *A. magnetotacticum* at (a) 80 and (b) 4.2 K. Note the reduction in the intensity of spectrum B at 4.2 K. (c) Cells at 4.2 K after anaerobic incubation above freezing temperature for 24 hours. Note enhancement of spectrum C at the expense of B. (Ref. 28).



to  $\text{Fe}_3\text{O}_4$  (spectra  $A_1$  and  $A_2$ ), a broadened quadrupole doublet with parameters characteristic of ferric iron (spectrum B), and a weak quadrupole doublet with parameters corresponding to ferrous iron (spectrum C). Spectra  $A_1$  and  $A_2$  correspond to  $\text{Fe}^{3+}$  in tetrahedral sites and  $\text{Fe}^{2+}$  and  $\text{Fe}^{3+}$  in octahedral sites in  $\text{Fe}_3\text{O}_4$ , respectively.<sup>29</sup>

Spectrum B was also observed in lyophilized cells and has isomer shift and quadrupole splitting parameters similar to iron in ferritin and in the mineral ferrihydrite, indicative of ferric iron with oxygen coordination. The relative intensity of B to  $A_1 + A_2$  was somewhat variable from sample to sample, depending on growth conditions. At 80 K, spectra  $A_1$  and  $A_2$  correspond to  $\text{Fe}_3\text{O}_4$  below the Verwey transition and the parameters of spectrum B and the relative intensity of B to  $A_1 + A_2$  are relatively unchanged compared to the spectrum at 250 K. Between 80 and 4.2 K, however, the intensity of B decreased with decreasing temperature so that at 4.2 K only a residual doublet remained. A similar temperature dependence for spectrum B was also obtained in lyophilized cells.

The isomer shift and quadrupole splitting parameters of spectrum C correspond to high spin ferrous iron in coordination with oxygen or nitrogen. This spectrum was not observed with lyophilized cells, possibly as a result of oxidation during sample preparation. Wet, packed cells kept unfrozen under anaerobic conditions contained increased amounts of material responsible for spectrum C and correspondingly less material with spectral characteristics B (Fig. 3b). Thawing and aeration of these frozen cells resulted in increases in B spectral lines and concomitant decreases in C spectral lines. This indicates that the iron atoms responsible for spectrum C came from reduction of the iron atoms giving spectrum B. Unlike that of spectrum B, the intensity of spectrum C did not decrease between 80 and 4.2 K (Fig. 3c).

The decrease in the intensity of spectrum B between 80 and 4.2 K can be explained as the onset of magnetic hyperfine interactions at low temperature resulting in a concomitant decrease in the intensity of the central absorption doublet, similar to ferritin. However, in the present case, the magnetic hyperfine lines were obscured by the magnetite spectral lines ( $A_1$  and  $A_2$ ). To further resolve the nature of the materials responsible for spectrum B, the temperature dependent Mössbauer spectra of nonmagnetotactic cells which lacked the interfering magnetite were studied.

For  $T \geq 80$  K, the spectrum of lyophilized nonmagnetotactic cells (Fig. 4) consisted primarily of the quadrupole doublet characteristic of ferric iron as denoted by spectrum B in Figs. 2 and 3. In addition, a very low intensity spectrum due to  $\text{Fe}_3\text{O}_4$  (spectral lines  $A_1 + A_2$  in Figs. 2 and 3) was observed. These latter spectral lines might have been due to a small fraction of magnetotactic cells in the sample or trace amounts of magnetite

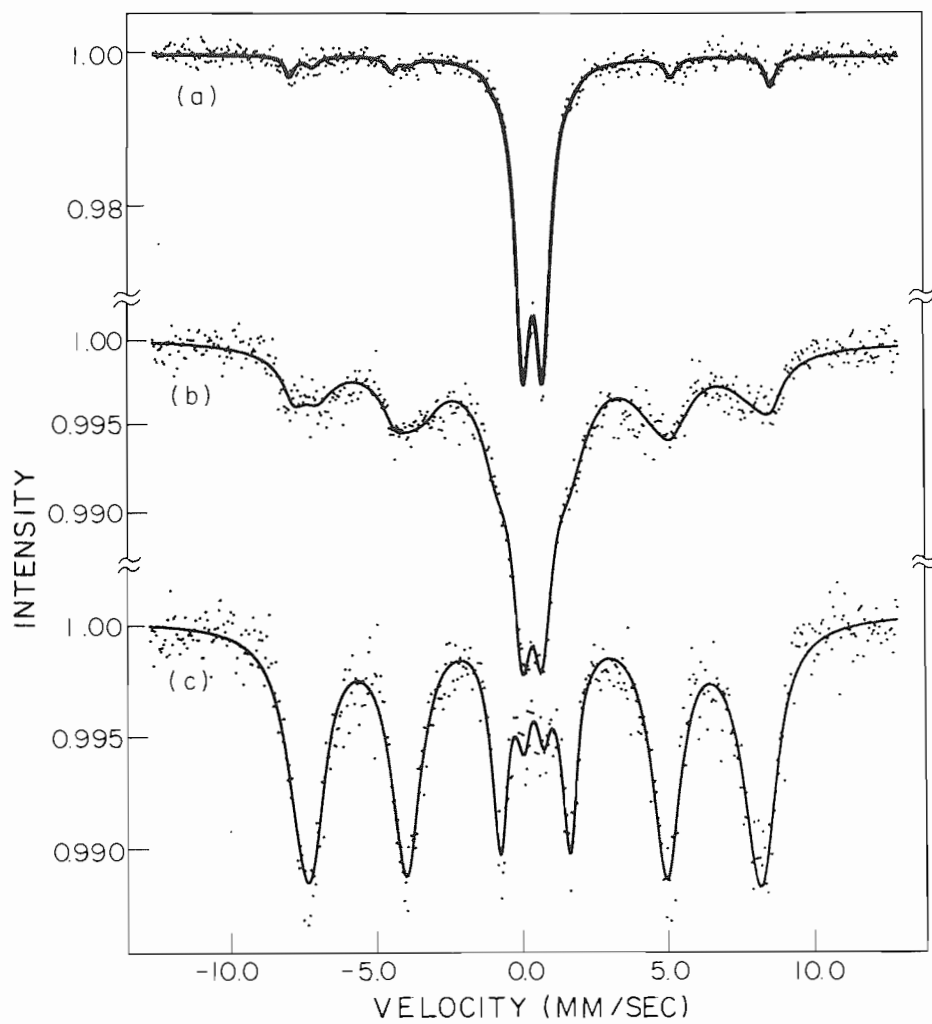


Fig. 4. Mössbauer spectra of nonmagnetic cells at (a) 100 K; (b) 40 K; (c) 4.2 K. (Ref. 28)

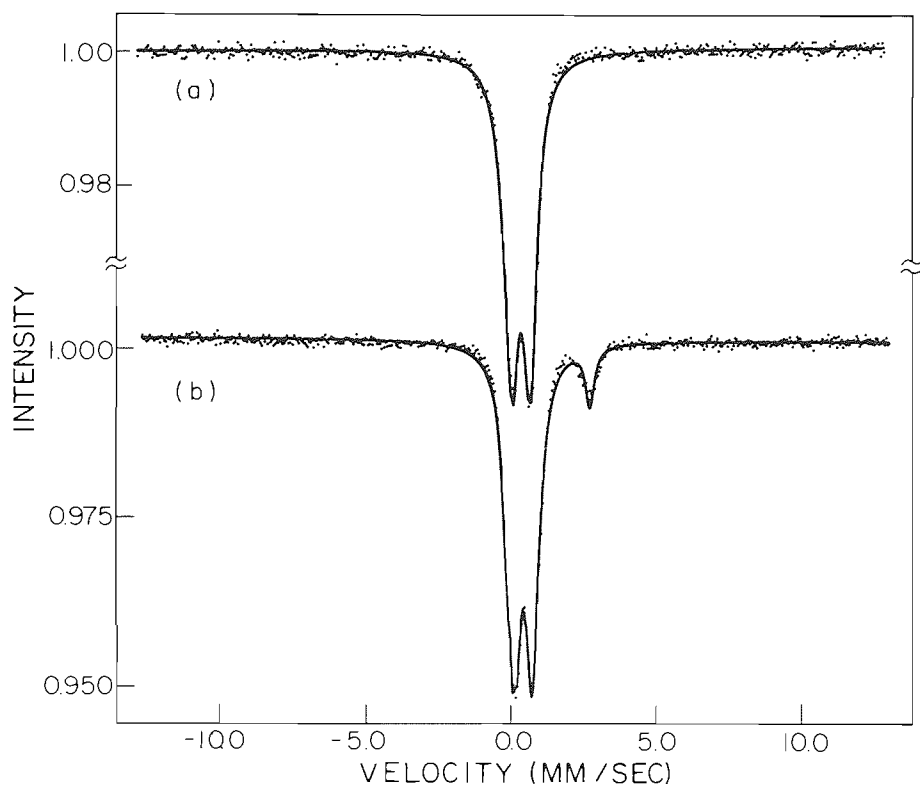


Fig. 5. Mössbauer spectra of a cloned, nonmagnetotactic strain at (a) 200 K; (b) 200 K following incubation above freezing temperature for 24 hours. (Ref. 28)

possibly present in the nonmagnetotactic cells. Below 80 K, the intensity of the quadrupole doublet decreased with decreasing temperature while the intensity of a six-line spectrum flanking the doublet increased. At 4.2 K the spectrum consisted primarily of the six broadened magnetic hyperfine lines, with a small residual doublet in the center. Spectral lines  $A_1 + A_2$  were obscured by the six-line spectrum. Application of a longitudinal magnetic field of 60 kOe produced broadening of the six-line spectrum but with no appreciable shifts in the line position and no decreases in any line intensities.

These spectral characteristics are indicative of small particles of hydrous-ferric-oxide with antiferromagnetic exchange interactions similar to those of the ferric iron within ferritin micelles. By comparison with ferritin, the experimental results indicate that hydrous-ferric-oxide particles in the nonmagnetotactic cells are of the order of 100 Å in diameter, or less. Unlike ferritin or ferrihydrite, however, there was a residual quadrupole doublet in the 4.2 K spectrum of magnetotactic and nonmagnetotactic cells. The intensity of this residual doublet varied somewhat from sample to sample, but its presence suggests another high spin ferric material with high temperature spectral characteristics similar to those of ferrihydrite, but with iron atoms less densely packed so that magnetic exchange interactions between them are weaker and the spectrum is not magnetically split at 4.2 K. This latter material was also observed in a cloned, nonmagnetotactic strain of A. magnetotacticum that accumulates less iron.

The Mössbauer spectrum of wet, packed cells of the cloned, nonmagnetotactic strain consisted of a quadrupole absorption doublet for  $T > 4.2$  K (Fig. 5). The spectral parameters obtained at 80 K were similar to those of spectrum B in magnetotactic cells, indicating the presence of a high spin ferric iron material. Application of an external 60 kOe magnetic field at 4.2 K results in spectra with a broad distribution of hyperfine fields. These spectral characteristics indicate the presence of high spin  $Fe^{3+}$  in a hydrous oxide with magnetic exchange interactions  $< 4$  K, that is, where the iron atoms are less densely packed than in ferrihydrite. This material has similar spectral characteristics to the iron storage materials in E. coli.<sup>14</sup>

When these wet, packed cells were held above 275 K in an anaerobic environment, a ferrous spectrum similar to spectrum C appeared, in addition to the ferric-iron doublet. This indicates that the hydrous-ferric-oxide in cells of this strain can be reduced to ferrous iron as with cells of the other strain.

In summary, cells of A. magnetotacticum contain ferrous ions, a low-density hydrous-ferric-oxide, a high-density hydrous-ferric-oxide (ferrihydrite) and  $Fe_3O_4$ . Additional experiments with cell

fractions show that ferrihydrite in the magnetotactic cells is associated with the magnetosomes.<sup>28</sup>

On the basis of the foregoing results it has been proposed<sup>28</sup> that A. magnetotacticum precipitates  $\text{Fe}_3\text{O}_4$  in the sequence:  $\text{Fe}^{3+}$  quinate  $\rightarrow \text{Fe}^{2+} \rightarrow$  low density hydrous-ferric-oxide  $\rightarrow$  ferrihydrite  $\rightarrow \text{Fe}_3\text{O}_4$ . In nonmagnetotactic cells the process stops with ferrihydrite. In cells of the cloned, nonmagnetotactic strain the process stops with low-density hydrous ferric oxide.

In the proposed process, iron enters the cell as  $\text{Fe}^{3+}$  chelated by quinic acid. Reduction to  $\text{Fe}^{2+}$  releases iron from the chelator.  $\text{Fe}^{2+}$  is reoxidized and accumulated as the low density hydrous-iron-oxide. By analogy with the deposition of iron in the micellar cores of the protein ferritin,<sup>7</sup> this oxidation step might involve molecular oxygen, which is required for  $\text{Fe}_3\text{O}_4$  precipitation in A. magnetotacticum.<sup>30</sup> Dehydration of the low-density hydrous-ferric-oxide results in ferrihydrite. Finally, partial reduction of ferrihydrite and further dehydration yields  $\text{Fe}_3\text{O}_4$ .

$\text{Fe}_3\text{O}_4$  is thermodynamically stable with respect to hematite and ferrihydrite at low  $E_H$  and high pH.<sup>31</sup> However, rapid transformation of ferrihydrite to magnetite appears to involve more than simple reduction and dehydration. While the degree of crystallinity of ferrihydrite can vary, in crystalline samples it has a structure related to hematite, with hexagonal close-packed oxygen atoms and  $\text{Fe}^{3+}$  octahedrally coordinated sites.  $\text{Fe}_3\text{O}_4$  has a cubic, inverse spinel structure with  $\text{Fe}^{3+}$  in octahedral and tetrahedral sites, and  $\text{Fe}^{2+}$  in octahedral sites. This, plus the fact that the precipitation process requires spatial segregation of regions of differing  $E_H$  and possibly pH, suggests that the process is organic matrix mediated. Thus the magnetosome envelope is probably an integral element in the precipitation process, functioning as a locus for enzymatic activities including control of  $E_H$  and pH, as well as a structural element.

The  $\text{Fe}_3\text{O}_4$  particles in A. magnetotacticum have also been studied by high resolution transmission electron microscopy.<sup>5</sup> The results show that many of the particles are well ordered single domain crystals with a distinct morphology. This is based on an octahedral prism truncated by {100} faces. The crystals are preferentially aligned with [111] direction parallel to the chain axis. This morphology is different from that of other magnetotactic bacterial particles.<sup>32</sup> Thus the morphology of  $\text{Fe}_3\text{O}_4$  particles produced by magnetotactic bacteria appears to be species specific.

No other crystalline phases were detected. However, in some crystals, noncrystalline material was found contiguous with the  $\text{Fe}_3\text{O}_4$ . This suggests that the hydrous-ferric-oxide phase is amorphous ferrihydrite,<sup>2</sup> and that deposition of  $\text{Fe}_3\text{O}_4$  occurs as a sol-

ution-reprecipitation process, possibly triggered by  $\text{Fe}^{2+}$  ions. 32,33

Finally, diffusive motions of the magnetosomes in A. magnetotacticum have been observed in the Mössbauer spectrum of the whole cells above 275 K.<sup>34</sup> The Mössbauer spectrum of the whole cells at  $T > 275$  K was dramatically different from that of the frozen cells ( $T < 265$  K)(Fig. 6). At 275 K it consisted primarily of a broad line of width  $\Gamma = 72 \pm 1$  mm/s. The width of the broad line increased with increasing temperature to  $\Gamma = 139$  mm/s at  $T = 295$  K (Fig. 7). However, the total spectral intensity was temperature independent and equal to the total spectral intensity of the sharp-line spectrum of the frozen cells. Some hysteresis in the solid-liquid transition was noted in spectra obtained at 270 K. If the sample temperature had been increased from 265 K, the sharp-line spectrum was observed. However, if the sample temperature had been decreased from 275 K the broad-line spectrum was obtained. For  $T > 275$  K, computer analysis showed that the intensity of the sharp-line  $\text{Fe}_3\text{O}_4$  spectrum superposed on the broad-line spectrum was less than 0.2%.

The temperature dependence of the additional quadrupole doublet depended on whether the iron was primarily  $\text{Fe}^{3+}$  or  $\text{Fe}^{2+}$ . When the additional iron was  $\text{Fe}^{3+}$ , as evidenced by the parameters of the doublet in the  $T = 265$  K spectrum, there was no residual doublet superposed on the broad-line spectrum at  $T > 275$  K. However, when the additional iron was primarily  $\text{Fe}^{2+}$ , the low intensity, sharp line  $\text{Fe}^{2+}$  doublet remained superposed on the broad-line spectrum.

The striking spectral change at 270 K can be explained by the onset of diffusive motions of the  $\text{Fe}_3\text{O}_4$  particles in the bacteria as they are warmed through the solid-liquid phase transition of the cytoplasmic fluid at 270 K.<sup>34</sup> Evidence for this comes from the fact that for freeze-dried cells the sharp-line spectrum persists at 300 K and the broad-line spectrum is never observed.<sup>22</sup> The broad-line spectra were analyzed with an extension of the "bounded diffusion" model previously developed for iron-containing proteins in the whole cells.<sup>16</sup> The analysis yielded the diffusion constant  $D$  of the magnetosomes, the effective viscosity  $\eta$  of the magnetosome environment, and the mean-squared translational displacements  $\langle x^2 \rangle < 8.4$  Å and rotational displacement  $\langle \theta^2 \rangle^{1/2} < 1.5$  Å. This implies that the particles are relatively fixed in the whole cells. The effective viscosity and diffusion constant are inversely proportional; at 295 K,  $\eta = 10$  cP and  $D = 96 \times 10^{-10}$  cm<sup>2</sup>/s.  $\eta$  has a temperature dependence similar to that of water.

The fact that the additional  $\text{Fe}^{3+}$  quadrupole doublet in the spectrum broadened together with the  $\text{Fe}_3\text{O}_4$  lines is consistent with the previous cell fractionation studies<sup>28</sup> that show the hydrous

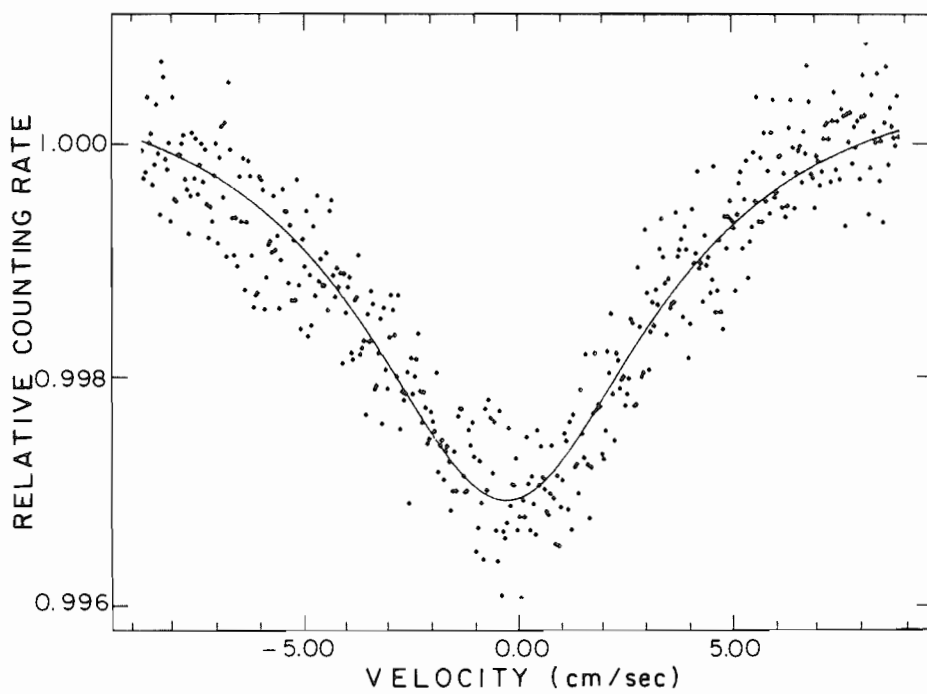


Fig. 6. Mössbauer spectrum of A. magnetotacticum at 275 K. (Ref. 34)

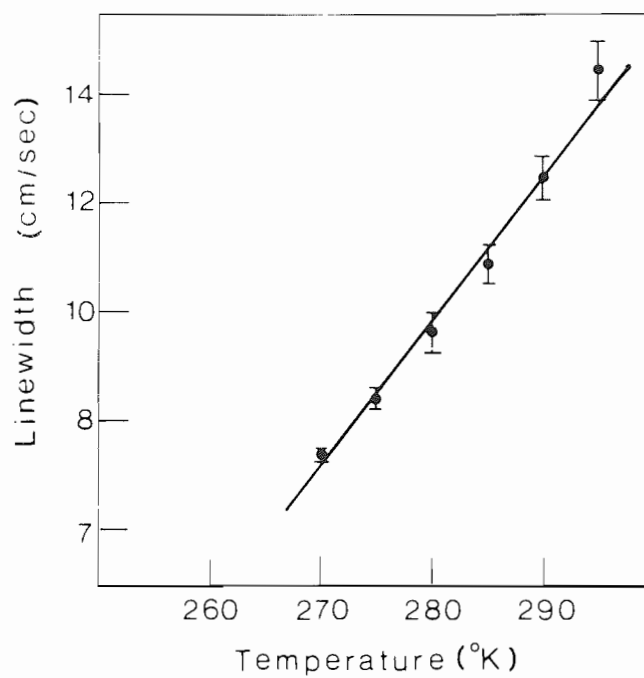


Fig. 7. Line width of the Mössbauer spectrum shown in Fig. 6 plotted as a function of temperature. (Ref. 34)



ferric-oxide to be primarily associated with the magnetosomes. Thus it undergoes the same diffusive motion as the magnetosomes. The fact that the sharp-line  $\text{Fe}^{2+}$  spectrum remains even when the  $\text{Fe}_3\text{O}_4$  lines have broadened shows that the  $\text{Fe}^{2+}$  material is not associated with the magnetosomes. If it was, or if the  $\text{Fe}^{2+}$  was dissolved in the cytoplasm, diffusive motion would broaden the sharp-line spectrum at  $T > 275 \text{ K}$ , contrary to experiment. This suggests that the  $\text{Fe}^{2+}$  is not associated either with the magnetosomes or with the cytoplasm in the cells. The  $\text{Fe}^{2+}$  is very probably associated with the peptidoglycan layer of the cell wall. This association could occur during the conversion from the iron quimate complex outside the cell to ferric iron and ultimately  $\text{Fe}_3\text{O}_4$  within the cell.

## CONCLUSION

Lowenstam<sup>2</sup> and Webb<sup>35</sup> have observed that biogenic iron oxides and oxyhydroxides are present in each of the five kingdoms of the biological world, with ferrihydrite the third more extensively formed mineral of biological origin and magnetite the fourth. Elucidation of the essentially bioinorganic processes of iron mineralization in organisms affords new opportunities for Mössbauer spectroscopy. We would like to understand how organisms accumulate and deposit iron minerals, with special emphasis on the mechanisms by which the deposition process is controlled.

## ACKNOWLEDGEMENT

We dedicate this paper to Solly G. Cohen and Shimon Ofer, our late friends and colleagues, and pioneers in Mössbauer spectroscopy. We thank R. Blakemore, W. O'Brien, S. Mann, I. Nowik, and E. R. Bauminger, for their contributions to the work reported here. This work was partially supported by the Office of Naval Research. The Francis Bitter National Magnet Laboratory is supported by the National Science Foundation.

## REFERENCES

1. A. Blaise, J. Chappert, and J. L. Giradet, 1965, Observation par mesures magnetiques et effet Mössbauer d'un antiferromagnetisme de grains fins dans la ferritine, C.R. Acad. Sci. Paris 261:2310-2313.
2. H. A. Lowenstam, 1981, Minerals formed by organisms, Science 211:1126-1130.
3. H. A. Lowenstam and S. Weiner, 1983, Mineralization by organisms and the evolution of biomineralization, in Biomineralisation and Biological Metal Accumulation, P. Westbroek and E. W. deJong, Eds., Reidel, Boston, 191-203.

4. R. P. Blakemore, 1975, Magnetotactic bacteria, Ann. Rev. Microbiol. 36:217-238.
5. S. Mann, R. B. Frankel, and R. P. Blakemore, 1984, Structure, morphology and crystal growth of bacterial magnetite, Nature (submitted).
6. H. L. Ehrlich, Geomicrobiology, (M. Dekkar, New York, 1981). 165-200.
7. G. A. Clegg, J. E. Fitton, P. M. Harrison, and A. Treffry, 1980, Ferritin: Molecular structure and iron-storage mechanisms, Prog. Biophys. Molec. Biol. 36:56-80.
8. K. M. Towe and W. F. Bradley, 1967, Mineralogical constitution of colloidal hydrous ferric oxides, J. Colloid. Interface Sci. 24:384-392.
9. F. V. Chukrov, B. B. Zvyagin, A. I. Gorshkov, L. P. Yermilova, and V. V. Balshova, 1973, Ferrihydrite, Int. Geol. Rev. 16: 1131-1143.
10. J. F. Boas and B. Window, 1966, Mössbauer spectroscopy of ferritin, Aust. J. Phys. 19:573-576.
11. W. T. Oosterhuis, K. Spartalian, 1976, Biological iron transport and storage compounds, in Applications of Mössbauer Spectroscopy, Vol. I (R. L. Cohen, Ed.), Academic Press, New York, 141-170.
12. J. M. Williams, D. P. Danson, and Chr. Janot, 1978, A Mössbauer determination of the iron core particle size distribution in ferritin, Phys. Med. Biol. 23:835-851.
13. E. I. Stiefel and G. D. Watt, Azotobacter cytochrome b<sub>557.5</sub> is a bacterioferritin, Nature, 279:81-83.
14. E. R. Bauminger, S. G. Cohen, D. P. E. Dickson, A. Levy, S. Ofer, and J. Yariv, 1980, Mössbauer spectroscopy of E. coli and its iron storage protein, Biochim. Biophys. Acta 623: 237-242.
15. S. G. Cohen, E. R. Bauminger, I. Nowik, and S. Ofer, 1981, Dynamics of the iron-containing core in crystals of the iron-storage protein, ferritin, through Mossbauer spectroscopy. Phys. Rev. Lett. 46:1244.
16. I. Nowik, S. G. Cohen, E. R. Bauminger, and S. Ofer, 1983, Mössbauer absorption in overdamped harmonically bound particles in Brownian motion, Phys. Rev. Lett. 50:1528-1530.
17. R. P. Blakemore, 1975, Magnetotactic bacteria, Science 190: 377-379.
18. R. P. Blakemore and R. B. Frankel, 1981, Magnetic navigation in bacteria, Sci. Am. 245:58-65.
19. T. T. Moench and W. A. Konetzka, 1978, A novel method for the isolation and study of a magnetotactic bacterium, Arch. Microbiol. 119:203-212.
20. D. L. Balkwill, D. Maratea, and R. P. Blakemore, 1980, Ultrastructure of a magnetotactic spirillum, J. Bacteriol. 141: 1399-1408.
21. K. M. Towe, and T. T. Moench, 1981, Electron-optical characterization of bacterial magnetite, Earth Planet. Sci. Lett. 52:213-220.

22. R. B. Frankel, R. P. Blakemore, R. S. Wolfe, 1979, Magnetite in freshwater magnetotactic bacteria, Science 203:1355-1356.
23. R. B. Frankel and R. P. Blakemore, 1980, Navigational compass in magnetic bacteria, J. Magn. and Magn. Mater. 15-18:1562-1564.
24. R. P. Blakemore, R. B. Frankel, A. J. Kalmijn, 1981, South-seeking magnetotactic bacteria in the Southern Hemisphere, Nature (London) 286:384-385.
25. J. L. Kirschvink, 1980, South-seeking magnetic bacteria, J. Exp. Biol. 86:345-347.
26. R. B. Frankel, R. P. Blakemore, F. F. Torres de Araujo, D. M. S. Esquivel, and J. Danon, 1981, Magnetotactic bacteria at the geomagnetic equator, Science 212:1269-1270.
27. R. P. Blakemore, D. Maratea, R. S. Wolfe, 1979, Isolation and pure culture of a freshwater magnetic spirillum in chemically defined medium, J. Bacteriol. 140:720-729.
28. R. B. Frankel, G. C. Papaefthymiou, R. P. Blakemore, and W. O'Brien, 1983, Fe<sub>3</sub>O<sub>4</sub> precipitation in magnetotactic bacteria Biochim. Biophys. Acta 763:147-159.
29. R. S. Hargrove, W. Kundig, 1970, Mössbauer measurements of magnetite below the Verwey transition, Solid State Commun. 8:303-308.
30. D. Bazylnski, R. P. Blakemore, R. B. Frankel, C. Rosenblatt, and K. Short, unpublished data.
31. R. M. Garrels and C. L. Christ, 1965, Solution, Minerals and Equilibria, Harper and Row, New York.
32. Y. Tamaura, K. Ito, and T. Katsura, 1983, Transformation of  $\gamma$ -FeO(OH) to Fe<sub>3</sub>O<sub>4</sub> by adsorption of iron (II) ion on  $\gamma$ -FeO(OH) J. Chem. Soc. Dalton Trans., 189-194.
33. S. Mann, T. T. Moench, R. J. P. Williams, 1984, A high resolution electron microscope investigation of bacterial magnetite; Implications for crystal growth, Proc. Roy. Soc. (in press).
34. S. Ofer, I. Nowik, E. R. Bauminger, G. C. Papaefthymiou, R. B. Frankel, and R. P. Blakemore, 1984, Magnetosome dynamics in magnetotactic bacteria, Biophys. J. (in press).
35. J. Webb, 1983, A bioinorganic view of the biological mineralization of iron in Biomineralization and Biological Metal Accumulation, P. Westbroek and E. W. deJong, Eds., Reidel, New York, 413-422.